

Anticancer Activities of Ag NPS Biosynthesized by Using Cassia Auriculata

M. Prem Nawaz^{1,2}, S. Raja Mohamed^{1,2}, V. Ramamurthy³, K. Mohamed Rafi⁴,
and A. Ayeshamariam^{1,5*}

¹Research And Development Center, Bharathidasan University, Tiruchirappalli, 620 024, India

²Department Of Chemistry, Khadir Mohideen College, Adirampattinam, 614701, India

³Department Of Biochemistry, Marudupandiyar College, Thanjavur, 613403, India

⁴Department Of Botany, Jamal Mohamed College (Auto), Tiruchirappalli, 620020, India

^{5*}Department Of Physics, Khadir Mohideen College, Adirampattinam, 614701, India

Corresponding Author: M. Prem Nawaz^{1,2}

Abstract: Cytotoxicity or cell viability of AgNPs have been prepared by silver nitrate by using the extract of *Cassia auriculata* leaves. The formation of dimensional structure of spherical nanoparticles with the addition of leaves extract prepared by using the 1Molar solution is prepared by using the reflux method. The crystal size of the Ag NPs was calculated and it is nearly 61 nm. When the *Cassia auriculata* leaves extract, it is used as reducing agent of Ag NPs and the morphology of Ag NPs have studied by using scanning electron microscopy and Transmission electron microscopy after calcinations at 350 °C. The anticancer activities of *Cassia auriculata* was studied for MCF7 cell line and was reported.

Keywords; *Cassia auriculata*, Ag NPs, MCF7 Cell line and Reflux method

Date of Submission: 13-08-2018

Date of acceptance: 30-08-2018

I. Introduction

A broad array of research activities that seek to develop new tools and techniques for the characterization and study of materials at the nanoscale and for the fabrication and processing of nanoscale devices and systems, these enabling nanoscale sciences and technologies include, in addition to the development of innovative approaches for ultra-high-resolution nanolithography and materials processing, the development of powerful, new scanned probe instruments for the measurement of electronic and magnetic properties at the nanoscale (Singh. M, 2008) [1]. Nanoparticle of gold, silver, copper, silicon, zinc, titanium, magnetite, palladium formation by plants has been reported. Colloid silver nanoparticle had exhibited distinct properties such as catalytic, antibacterial (Sharma et al., 2009) [2], good conductivity and chemical stability. Silver nanoparticles have its application in the field of bio labelling, sensor, antimicrobial, catalysis, electronic and other medical application such as drug delivery (De Jong, W.H et al., 2008) [3] and disease diagnosis. There have also been several experiments performed on the synthesis of silver nanoparticles using medicinal plants such as *Oryza sativa*, *Helianthus annuus*, *Saccharum officinarum*, *Sorghum bicolor*, *Zea mays*, *Basella alba*, *Aloe vera*, *Capsicum annuum*, *Magnolia kobus*, *Medicago sativa*, *Cinamomum camphora* and *Geranium sp.* in the field of pharmaceutical applications and biological industries. Besides, green synthesis of Ag-NPs using an extract of *Eucalyptus hybrida* was also investigated (Kasthuri et al., 2009) [4].

Exposure to free radicals from a variety of sources has led to the evolution of a series of defense mechanisms in organisms. Defense mechanisms against free radical-induced oxidative stress include: (i) preventive mechanisms, repair mechanisms, (iii) physical defenses and (iv) antioxidant defenses. Enzymatic antioxidant defenses include three primary enzymes, namely superoxide dismutase (SOD), catalase (CAT), and glutathione peroxidase (Gpx), which are involved in direct elimination of ROS, and secondary enzymes, namely glutathione reductase (GR), glutathione-S-transferase (GST), glucose-6-phosphate dehydrogenase (G6PDH), and ascorbate peroxidase (Apx), which help in the detoxification of ROS by decreasing peroxide levels or by maintaining a steady supply of metabolic intermediates (glutathione, NADPH) that are necessary for optimum functioning of the primary antioxidant enzymes (Singh et al., 2003) [5]. Non-enzymatic antioxidants are represented by ascorbic acid (vitamin C), α -tocopherol (vitamin E), glutathione (GSH), carotenoids, flavonoids, and other antioxidants which as a whole, play a homeostatic or protective role against ROS. Silver nanoparticles with their unique chemical and physical properties are proving to be an alternative for the development of new pharmacological agents. Silver nanoparticles have also found diverse applications in the form of wound dressings, coatings for medical devices and silver nanoparticle impregnated textile fabrics, etc.

(Rai *et al.*, 2009) [6]. The UV absorption peak of silver nanoparticles ranges from 400 nm – 450 nm. The UV absorption peak of silver nanoparticles range was from 400 nm – 450 nm. The occurrence of the peak at 421 nm is due to the phenomenon of surface Plasmon resonance, which occurs due to the excitation of the surface plasmons present on the outer surface of the silver nanoparticles which gets excited due to the applied electromagnetic field (Sonali Pradhan, 2013) [7]. Silver nanoparticles exhibited yellowish brown color in aqueous solution due to excitation of surface plasmon vibrations in silver nanoparticles (Jancy Mary and Inbathamizh, 2012). Absorption spectra of silver nanoparticles formed in the reaction media had absorbance peak at 430 nm and the broadening of peak indicated that the particles were polydispersed [8]. Silver ions were reduced to silver nanoparticles when added to *Cassia auriculata* plant powder. In *Cassia auriculata* before addition of AgNO₃ its colour was red but after its treatment with AgNO₃ its colour changes to dark brown which indicated the formation of silver nanoparticles. This colour change is due to the property of quantum confinement which is a size dependent property of nanoparticles which affects the optical property of the nanoparticles. (Krishnaraj *et al.*, 2010) [9]. The usage of MCF-7 breast cancer cell lines is widely used nowadays in numerous researches for the anticancer properties. MCF-7 cells are the most commonly used model of estrogen positive breast cancer. The VERO cell is a normal mammalian cells extracted from African green monkey kidney which is generally used in pharmaceutical research [10].

II. Experimental

The *Cassia auriculata* leaf was collected, washed, cut into small pieces and dried at room temperature (28±1°C) for two weeks and made into fine powder for further analysis. The shade-dried leaf powder of *Cassia auriculata* were subjected to extraction with 70% ethanol under reflux for 8 h and concentrated to a semisolid mass under reduced pressure (Rotavapor apparatus, Buchi Labortechnik AG, Switzerland). A dark semisolid (greenish-black) material was obtained and the yield was about 24% (w/w). It was stored at 4° C until used. When needed, the residual extract was suspended in distilled water and used for the study. The leaves powder of *Cassia auriculata* was taken in an apparatus and refluxed serially using solvent systems (95% ethanol and water) depending upon the polarity. The extracts solvent system was concentrated (by evaporation) separately in previously weighed beaker. Antimicrobial activities of *Cassia auriculata* have been studied

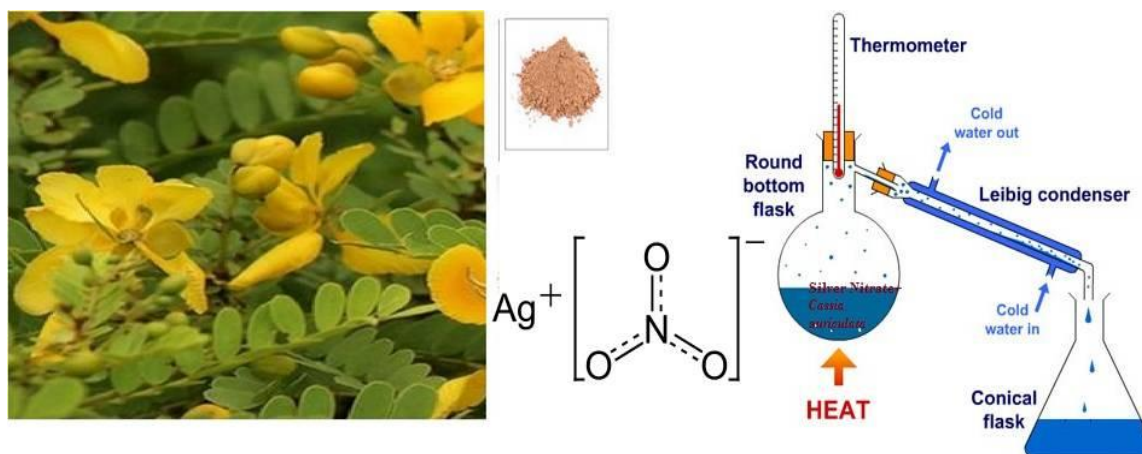


Figure 1 Preparation of Ag NPs by using *Cassia auriculata* leaves extract by reflux method

Open reflux method is used to prepare the Ag NPs, with 1 molar solution of standard silver nitrate and leaves extract were refluxed in strongly with phosphoric acid for 2 hrs using a reflux apparatus comprising of an Erlenmeyer flask, a vertical condenser and heating mantle. The silver nitrate reduced solution of the leaves extract are measured by using this indicator. The mother solution has the strong reducing agent under acidic conditions. Acidity is usually achieved by the addition of phosphoric acid. For all organic matter to be completely reduced, an excess amount of extract must be evaporated. Once reducing is complete, the amount of silver must be ensured which can be annealed at 350° C for one hour further shown in Figure 1[11].

2.1 Characterization Technique

The X-ray powder diffraction (XRD) experiments were measured on a Rigaku D/max-RB diffractometer with Ni-filtered graphite monochromatized CuK_α radiation (λ = 1.54056 Å) under 40 kV, 30 mA and scanning between 10° to 90° (2θ). The morphology was characterized by scanning electron microscopy (SEM, Hitachi, S-4800) and transmission electron microscopy (TEM, Tecnai G2, FEI Company) with X-ray energy dispersive spectrometry (EDS). Fourier transform infrared spectrum (FTIR) was recorded on a Nicolet

NEXUS 670 FTIR spectrometer. And the PL spectra were recorded using an FLS-920T fluorescence spectrophotometer equipped with a 450 W Xe light source and double excitation monochromators.

III. Results and Discussion

3.1 XRD Analysis

Further studies using XRD were carried out to confirm the crystalline nature of the particles, and the XRD pattern showed the number of Bragg's reflections that may be indexed on the basis of the face centered cubic structure of silver. PAN Analytical X-ray diffractometer is used to find the diffraction planes of the crystals. Figure 2 shows a XRD diagrams for the annealed NPs at 350° C synthesized by using Cassia auriculata leaves extract. We observe a preferred growth orientation of the Ag NPs, following the a-axis 65-2871 JCPDS values denoting the structure of the NPs, we used the Scherrer's formula to calculate the crystal size, its value was nearly 61 nm,

$$D = \left(\frac{0.94\lambda}{\beta \cos\theta} \right)$$

With β , the peak width at half height expressed in radians and θ , the diffraction peak position observed. Ag NPs has a cubic structure and its d_{hkl} spacing is expressed as

$$a = \left(d_{hkl} \sqrt{h^2 + k^2 + l^2} \right)$$

Lattice constant 4.112 the experimental and calculated values were listed in Table -1,

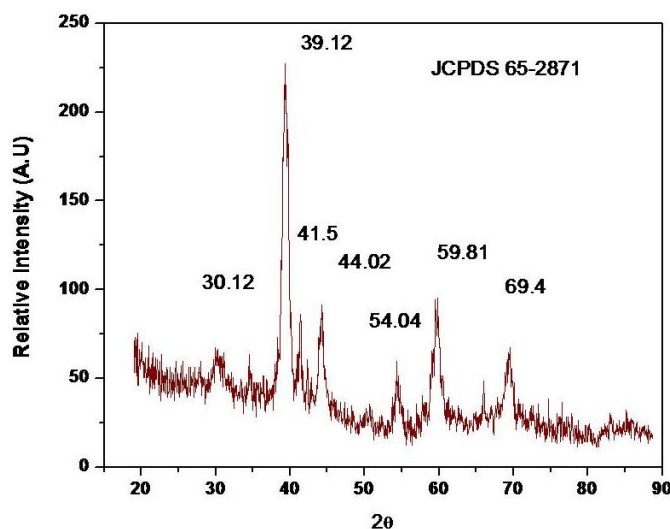


Figure 2 XRD Analysis of Ag NPs using Cassia auriculata

Table -1 Strutural parameter of Ag NPs synthesized by using Cassia auriculata

JCPDS 65-2871	2θ	d-spacing	Crystal size (nm)	Lattice constant (Å)
Standard from JCPDS	38.116	2.3591	61	4.086
Calculated	39.120	2.395		4.112

3.1 Analysis of Cassia auriculata leaf by GC-MS

Use of GC/MS enabled identification of the most components in leaves samples of *Cassia auriculata* were analyzed by phyto constituents. The compounds identified are listed in Table 2. The natural compounds have been a source of medicinal agents for hepatoprotective, antimicrobial, anti-inflammatory properties. Essential fatty acids and some alkaloids, flavonoids and phenol are analyzed in this plant. The components of the infusion differ from those found in tincture except organic acids derivatives. The concentrations (in %MS) of these derivatives in infusion and tincture are a great deal closed; maybe that is why in traditional medicine both types of extracts are used with success. Twenty eight compounds were identified in *Cassia auriculata* leaf extract by GC-MS analysis [12]. The chromatogram is obtained by fraction of *Cassia auriculata*. The active principle, area of the peak, height (%), Retention Time (RT), molecular formula and molecular weight were varied. The prevailing compounds were Resorcinol, 1-butanol, 3-methyl-, acetate, 2,3-dihydro-benzofuran, 1-Heptacosanol, Stigmast-5-En-3-Ol, (3.Beta.)-. Stigmasterol, 3-[(trimethylsilyl) oxy]phenol, xanthosine etc. The analytical methods GC/MS is suitable for medicinal herbs organic compounds determination. The sample preparation method is rapid and precise. There is a difference between the compounds extracted from herbs by

infusion and tincture but the important thing is that the organic acid and fatty acids derivatives are present in both of them. In the flower extracts organic acid derivatives and vitamins (polyunsaturated fatty acids) are present in very high amount. In conclusion flavonoids, terpenic compounds, fatty acids, phytol, alkaloids and especially organic acid derivatives are responsible for the therapeutic activity of this plant shown in Figure 3.

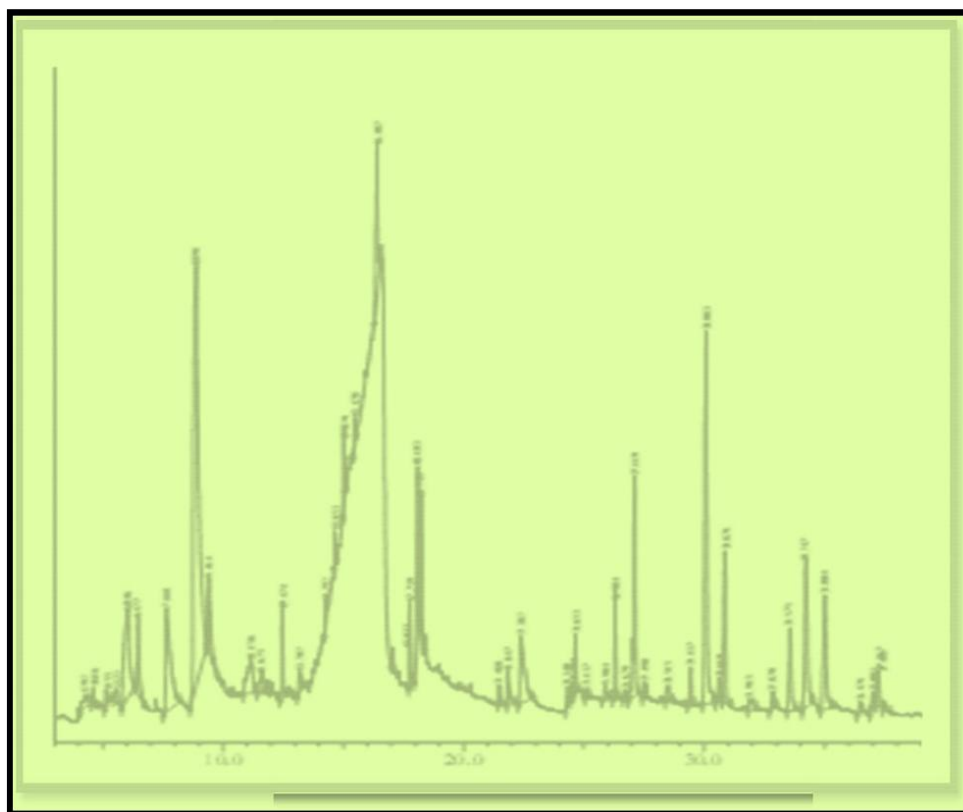


Figure 3 GCMS chromatogram of dried leaves of *Cassia auriculata*

Table 2 Some mineral element compositions of *Cassia auriculata* leaves

S. No	Elements	Concentration (ppm)
1	Iron (Fe)	171.3 ± 0.12
2	Zinc (Zn)	56.8 ± 0.47
3	Magnesium (Mg)	172.5 ± 0.38
4	Calcium (Ca)	313.1 ± 0.16
5	Manganese (Mn)	34.25 ± 0.21
6	Potassium (K)	710.3 ± 0.39
7	Sodium (Na)	619.1 ± 0.35
8	Phosphorus (P)	92.32 ± 0.17

3.3 SEM Analysis

A scanning electron microscope was employed to analyze the shape of the silver nanoparticles that were synthesized by green method. Scanning electron microscopy of pure *Cassia auriculata* leaves extract powder were spherical in size in the size of micrometer shown in Figure 4a. SEM analysis of Ag NPs showed that the *Cassia auriculata* have tremendous capability to synthesize silver nanoparticles which were roughly spherical in shape, Figure 4b was uniformly distributed, and its size reduced to when compared with pure extract powder. Ag NPs by using *Cassia auriculata* has small in size of nm and Ag NPs EDAX analysis was shown in Figure 4c.

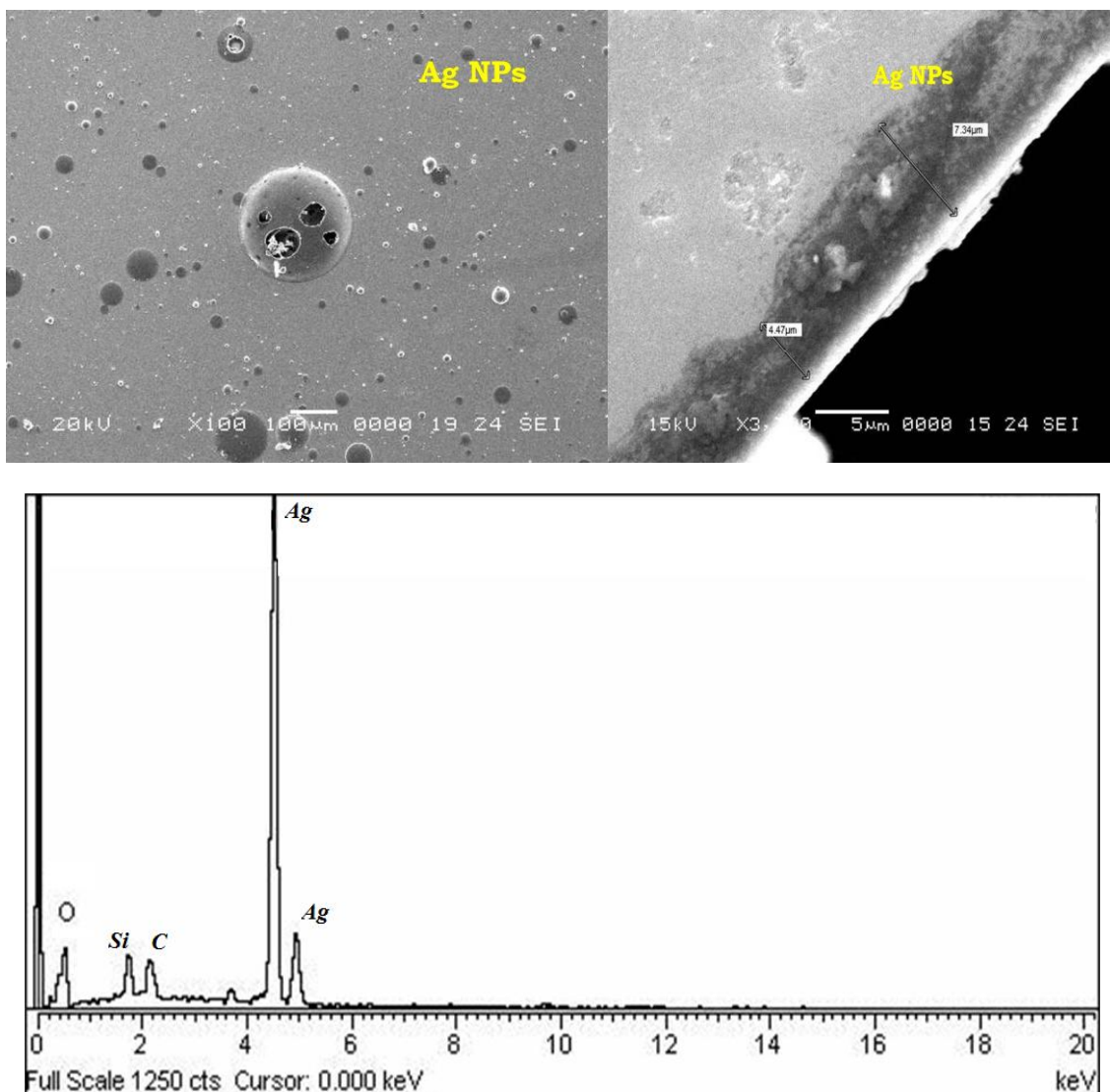


Figure 4(a-c) SEM analyses of dried leaves of *Cassia auriculata* and Ag NPs and its EDAX of Ag NPs

3.4 TEM Analysis

The TEM images indicated equally spherical shaped orthorhombic crystals. Colloidal silver nanoparticles from *Cassia auriculata* were analyzed using transmission electron microscopy (TEM), by drying a drop of the washed colloidal dispersion onto a copper grid covered with a conductive polymer. The size and shape of Ag nanoparticles synthesized using *Cassia auriculata* leaf was visualized using 200 kV Ultra High Resolution TEM. Previous report of TEM analysis of biogenic Ag nanoparticles prepared by *Cassia auriculata* extract shows that the size measurement of the particle was found to 30 – 40 nm in diameter the decrease in anisotropy and particle size was evident from the images. The TEM image of Ag NPs synthesized by using *Cassia auriculata* leaf extract which predominates with spherical triangle, truncated triangles, and decahedral morphologies ranging from 30 to 40 nm with an average size of 28.40 nm. Most of the AgNPs were roughly circular in shape with smooth edges. These structures were identical with those of the Ag nanoparticles produced from the extract prepared from leaves of *Cinnamomum camphora* and phyllanthin, which was attributed to a similarity in the reductive agents present in both plant species [13] shown in Figure 5(a-b).

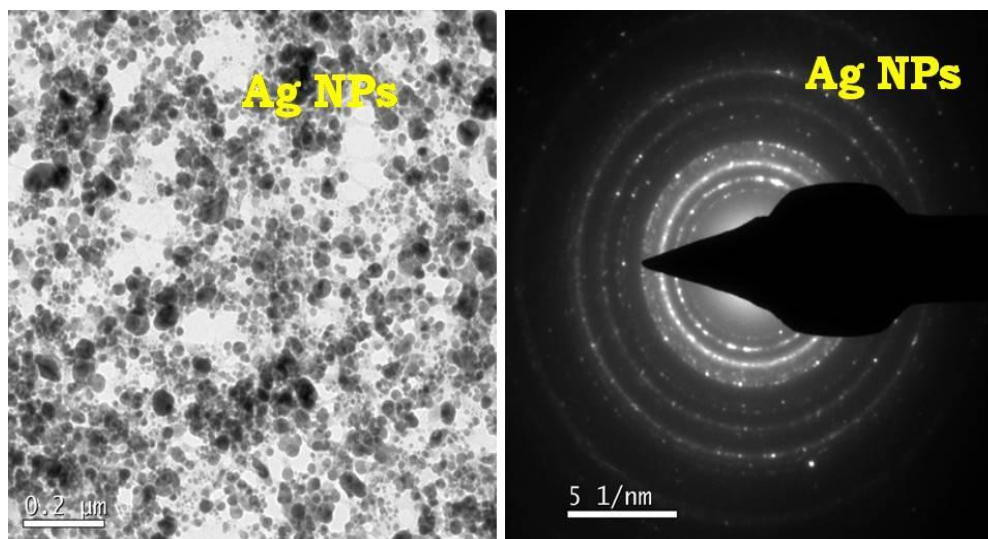


Figure 5(a-b) TEM and SAED pattern analysis of Ag NPs prepared by using *Cassia auriculata*

3.5 Cytotoxicity Effect

In the silver nanoparticle study, the maximum cell inhibition (90.42 %) and minimum cell viability (9.58 %) were noted in the 100 $\mu\text{g/ml}$ concentration of silver nanoparticle against MCF-7 cell line and minimum cell inhibition (26.72 %) and maximum cell viability (73.28 %) were observed in the 0.78 $\mu\text{g/ml}$ concentration of the silver nanoparticles. Natural derivatives play an important role to prevent the cancer incidences as synthetic drug formulations cause various harmful side effects to human beings. The characteristic condensation pattern observed were the crescent shape at the nuclear periphery and the more numerous round clumps. The *invitro* cytotoxicity was meant to determine the IC_{50} of the crude sample towards to the cells. It is evident that the acetone extracts of *H. pinifolia* exhibited less prominent antiproliferative activity on the Vero cell line. The extracts mediated antiproliferative activity is limited to the cancer cell lines rather than the normal cell lines. This indicates that the specific inhibitory effect may be due to the apoptosis-inducing ability of the acetone extracts of *H. pinifolia* in response to the defective gene expression in cancer cell lines rather than the normal cell line. With the significant antiproliferative activity of the extracts of plant against MCF-7 cancer cell lines, the mechanisms of action could, possibly, be due to the dose-dependent apoptosis-inducing ability, by necrosis of cancer cell lines, by enhanced neoplastic transformation followed by apoptosis or by any other mechanisms related to epigenetic and signal transduction pathways. Phytochemicals such as vitamins (A, C, E, and K), carotenoids, terpenoids, flavonoids, polyphenols, alkaloids, tannins.

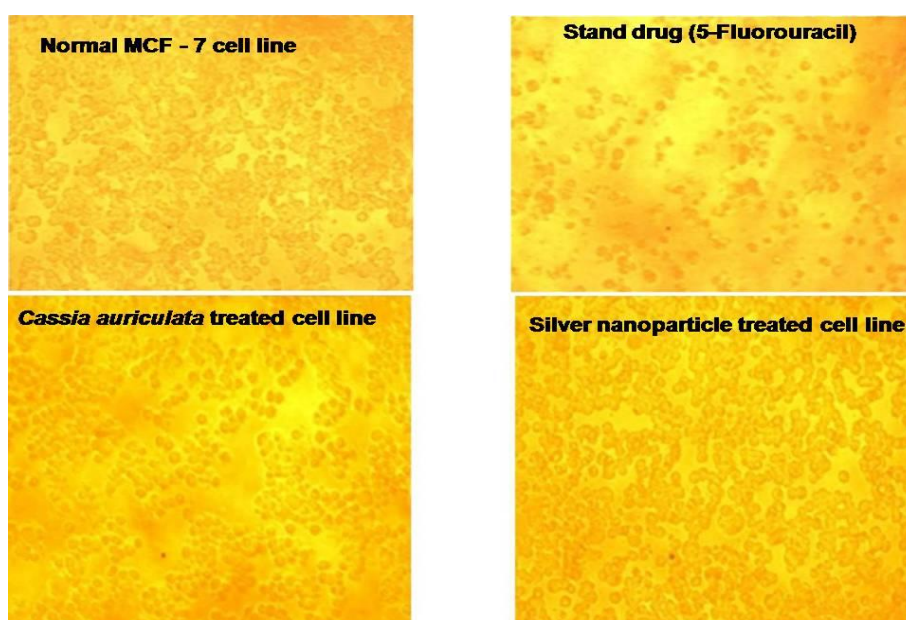


Figure 6(a-d) Plate showing the anticancer activity of MCF-7 cell line of silver nanoparticles *Cassia auriculata* leaf extracts

3.6 DMSO act as a vehicle control and it had 100% cell viability in all the cell lines.

Breast cancer is the leading cause of death among women in many countries (Giaciniti *et al.*, 2006) [14]. Although male breast cancer is less common, a few studies have revealed that the incidence has increased over the past 25 years (Sanguinetti *et al.*, 2014) [15]. Scientists have aimed to treat breast cancer without harming the patient by exploiting the differences between cancerous and normal cells. Nutritional strategies have been applied to study populations with a low incidence of breast cancer. In Asia, seaweeds have been eaten for at least 5000 years (Liu *et al.*, 2012) [16].

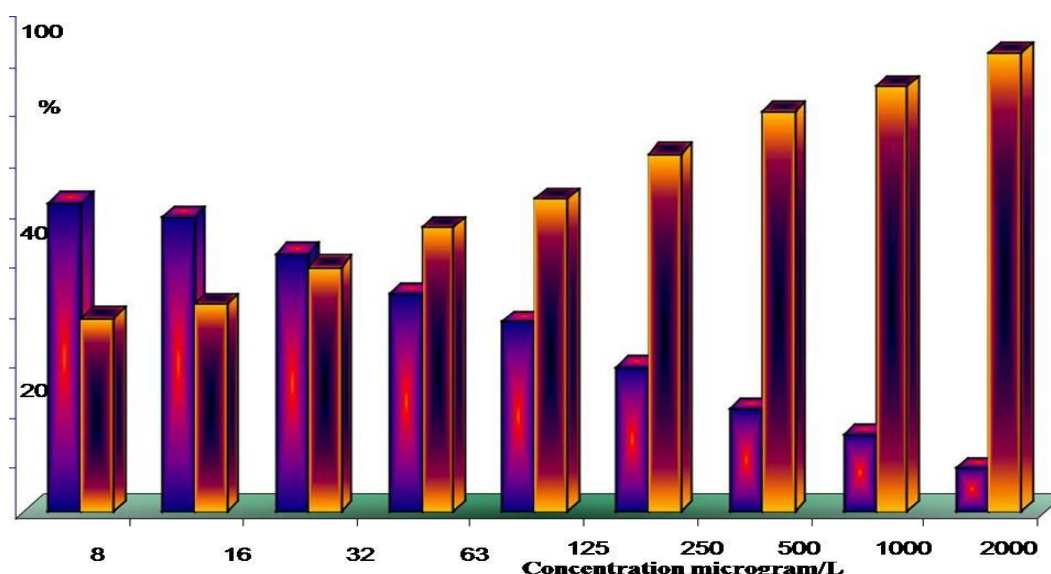


Figure 7 Bar diagram showing the Anticancer ethanolic extract of *Cassia auriculata* on MCF-7 cell line

These populations have a low incidence of breast cancer. Certain brown and red algae are known for their anticancer properties (Khan *et al.*, 2012) [17]. In cells treated with seaweed, apoptosis was observed (Funahashi *et al.*, 2001) and the authors speculated that seaweed could be a breast cancer-preventing food [18]. Some studies recently evaluated the effect of a brown seaweed (*Sargassum muticum*) methanol extract (SMME) on the proliferation of MCF-7 and MDA-MB-231 breast cancer cell lines (Namvar *et al.*, 2013) [19], by conducting morphological assessments of apoptosis, caspase assays, and chick chorioallantoic membrane (CAM) assays. The present study suggested that the minimum cell viability (11.54 %) and maximum cell inhibition (88.46 %) were noted in 1000 µg ml⁻¹ concentration of *S. isoetifolium* and followed by 500 µg ml⁻¹ concentration also recorded in the maximum cell inhibition (82.7 %) (Table.3) against MCF-7 cell line shown in Figure 6(a-d)

Table -3 Anticancer activity ethanolic extract of *Cassia auriculata* on MCF-7 cell line

Concentrations (µg ml ⁻¹)	Cell viability (%)	Cell inhibition (%)	IC 50 (µg ml ⁻¹)
7.8	61.52	38.48	84.56
15.6	58.78	41.32	
31.2	51.29	48.71	
62.5	43.33	56.67	
125	37.55	62.45	
250	28.82	71.18	
500	20.21	79.79	
1000	15.46	84.54	
2000	8.75	91.25	
Vehicle control (DMSO)	100	0	

3.7 MCF7 cell line (Breast cancer cell)

The minimum cell viability (8.75%) and maximum cell inhibition (91.25%) were noted in 2000 µg/ml concentration of *Cassia auriculata* extract and followed by 1000 µg/ml concentration also recorded in the maximum cell inhibition (84.54%) (Table 4). The moderate levels of cell inhibition (56.67%, 62.45%, 71.18 and

79.79%) were observed in the different concentrations of ethanolic extract of *C. auriculata* in 62.5µg/ml, 125µg/ml, 250 µg/ml and 500µg/ml respectively shown in the bar chart Figure 7. The IC₅₀ value was noted in the concentration of 84.56 µg/ml against the MCF7 anticancer activity of ethanolic leaves extract of *C. auriculata*. In the standard, the minimum cell viability and maximum cell inhibition were observed in higher concentration (1000 µg/ml). The IC₅₀ value 14.7µg/ml was showed the standard 5-Fluorouracil against MCF-7 cell line. It is interesting that the traditional method of treating a microbial infection was by administering a decoction of the plant, whereas according to our results an ethanolic extract was better; hence this may be more beneficial. Amongst the six bacterial and three fungal strains investigated that the *H. pylori* is the more resistant and *T. viride* is less resistant.

IV. Conclusion

From XRD analysis it was concluded that the nanoparticles were crystalline in nature having cubical shape with no such impurities. Twenty eight compounds were identified in *Cassia auriculata* leaf extract by GC-MS analysis. The chromatogram is obtained by fraction of *Cassia auriculata*. FTIR gives the information about functional groups present in the synthesized silver nanoparticles for understanding their transformation from simple inorganic AgNO₃ to elemental silver by the action of the different phytochemicals which would act simultaneously as reducing, stabilizing and capping agent. The anticancer activities of *Cassia auriculata* were studied in different MCF7 cell line. The present investigation different concentration of ethanolic extract of *Cassia auriculata* used against in MCF7 cell lines also compare with standard drug determined by MTT assay. The minimum cell viability and maximum cell inhibition were noted in 2000 µg concentration of *Cassia auriculata*. IC₅₀ value (98.41 µg/ml) was calculated for anticancer activity of ethanolic extract of *Cassia auriculata* against MCF7 cell line. The percentage of cell inhibition was noted in the different concentrations of silver nanoparticle of *Cassia auriculata* ranges from 0.78 to 100 µg/ml. The lowest cell inhibition (16.56%) was recorded in the lowest concentration and highest cell inhibition (74.80%) was noted in the higher concentration of silver nanoparticles

References

- [1]. Singh, M., Singh, S., Prasad, S. and Gambhir, I.S., Nanotechnology in medicine and antibacterial effect of silver nanoparticles. Digest Journal of Nanomaterials and Biostructures, 2008, 3(3), 115-122.
- [2]. Sharma A, Tyagi VV, Chen CR, Buddhi D. Review on thermal energy storage with phase change materials and applications. Renewable and Sustainable energy reviews. 2009, 1;13(2):318-45.
- [3]. De Jong, W.H. and Borm, P.J., Drug delivery and nanoparticles: applications and hazards. International journal of nanomedicine, 2008, 3(2), 133.
- [4]. Kasthuri, R.S., Taubman, M.B. and Mackman, N., Role of tissue factor in cancer. Journal of Clinical Oncology, 2009, 27(29),4834.
- [5]. Singh, S.K., Clarke, I.D., Terasaki, M., Bonn, V.E., Hawkins, C., Squire, J. and Dirks, P.B., Identification of a cancer stem cell in human brain tumors. Cancer research, 2003,63(18), 5821-5828.
- [6]. Rai, M., Yadav, A. and Gade, A., Silver nanoparticles as a new generation of antimicrobials. Biotechnology advances, 2009, 27(1), pp.76-83.
- [7]. Pradhan, S., Comparative analysis of Silver Nanoparticles prepared from Different Plant extracts (*Hibiscus rosa sinensis*, *Moringa oleifera*, *Acorus calamus*, *Cucurbita maxima*, *Azadirachta indica*) through green synthesis method(Doctoral dissertation), 2013.
- [8]. Jancy, M.E. and Inbathamizh, L., Green synthesis and characterization of nano silver using leaf extract of *Morinda pubescens*. Asian J Pharm Clin Res, 2012, 5(1), 159-162.
- [9]. Krishnaraj C, Jagan EG, Rajasekar S, Selvakumar P, Kalaichelvan PT, Mohan N. Synthesis of silver nanoparticles using *Acalypha indica* leaf extracts and its antibacterial activity against water borne pathogens. Colloids and Surfaces B: Biointerfaces. 2010 , 1;76(1):50-6.
- [10]. Kasthuri, J., Veerapandian, S. and Rajendiran, N., Biological synthesis of silver and gold nanoparticles using apiin as reducing agent. Colloids and Surfaces B: Biointerfaces, 2009, 68(1), pp.55-60.
- [11]. Kaviyarasu, K., N. Geetha, K. Kanimozhi, C. Maria Magdalane, S. Sivarajani, A. Ayeshamariam, J. Kennedy, and M. Maaza. "In vitro cytotoxicity effect and antibacterial performance of human lung epithelial cells A549 activity of zinc oxide doped TiO₂ nanocrystals: investigation of bio-medical application by chemical method." Materials Science and Engineering: (2017), C 74, 325-333.
- [12]. Thirumalairajan, S., Girija, K., Hebalkar, N.Y., Mangalaraj, D., Viswanathan, C. and Ponpandian, N., Shape evolution of perovskite LaFeO₃ nanostructures: a systematic investigation of growth mechanism, properties and morphology dependent photocatalytic activities. RSC Advances, 2013, 3(20),7549-7561.
- [13]. Hakkim, F.L., Arivazhagan, G. and Boopathy, R., Antioxidant property of selected *Ocimum* species and their secondary metabolite content. Journal of Medicinal Plants Research, 2013, 2(9), 250-257.
- [14]. Giacinti C, Giordano A. RB and cell cycle progression. Oncogene. 2006, 25(38):5220.
- [15]. Sanguinetti B, Martin A, Zbinden H, Gisin N. Quantum random number generation on a mobile phone. Physical Review X. 2014, 29;4(3):031056.
- [16]. Liu B. Sentiment analysis and opinion mining. Synthesis lectures on human language technologies. 2012, 22;5(1):1-67.
- [17]. Khan AS, Yu S, Liu H. Deformation induced anisotropic responses of Ti-6Al-4V alloy Part II: A strain rate and temperature dependent anisotropic yield criterion. International Journal of Plasticity. 2012, 1;38:14-26.
- [18]. Weyer C, Funahashi T, Tanaka S, Hotta K, Matsuzawa Y, Pratley RE, Tataranni PA. Hypoadiponectinemia in obesity and type 2 diabetes: close association with insulin resistance and hyperinsulinemia. The Journal of Clinical Endocrinology & Metabolism. 2001, 1;86(5):1930-5.
- [19]. Namvar, F., Mohamad, R., Baharara, J., Zafar-Balanejad, S., Fargahi, F. and Rahman, H.S., Antioxidant, antiproliferative, and antiangiogenesis effects of polyphenol-rich seaweed (*Sargassum muticum*). BioMed research international, 2013.